Proceedings of the 4th WSEAS International Conference on Fluid Mechanics and Aerodynamics, Elounda, Greece, August 21-23, 2006 (pp376-383)

Comparison of a two-dimensional viscid and inviscid model for rotating stall analysis

S. LJEVAR, H.C. DE LANGE, A.A. VAN STEENHOVEN
Department of Mechanical Engineering
Eindhoven University of Technology
Den Dolech 2, 5600 MB Eindhoven
THE NETHERLANDS

Abstract: - A two-dimensional numerical analysis of the vaneless diffuser core flow, where the influence of the wall boundary layers is neglected, is performed to investigate the rotating stall instability. A commercial code with the standard incompressible viscous flow solver is applied to model the vaneless diffuser core flow in the plane parallel to the diffuser walls. At the diffuser inlet a rotating jet-wake velocity pattern is prescribed, and at the diffuser outlet a constant static pressure is assumed. With this model a two-dimensional rotating instability was obtained, which is associated with the rotating stall instability in wide vaneless diffusers. In this paper it is shown that the number of rotating cells is dependent of the diffuser geometry, and that the maximum number of rotating cells observed in the vaneless diffuser space can be estimated. This two-dimensional numerical model is compared with the two-dimensional inviscid flow model of the vaneless diffuser rotating stall based on instability analysis. Similar results are obtained with both models for the critical flow angle, number of rotating cells and their propagation speed.

Key-Words: - centrifugal compressor, core flow, rotating stall, vaneless diffuser, instability

1 Introduction

The performance of centrifugal compressors at low mass flows is characterized by the occurrence of unsteady flow phenomena. Rotating stall is an instability with strong dynamical loading on the blades that can cause damage and noise nuisance. Therefore, it can not be tolerated during compressor operation. Limited compressor operating range is paid with the loss of high-pressure ratios. To increase the efficiency of compressors, a lot of effort is made to postpone the unsteady flow phenomena as much as possible. In order to increase the region of operation of centrifugal compressors the understanding of rotating stall flow dynamics is required.

This paper deals with the study of rotating stall instability within the vaneless radial diffusers. In [1-3] was found that vaneless diffuser performance is different for narrow and wide diffusers, and it is clearly suggested that different flow mechanisms might exist that can lead to the occurrence of rotating stall. Generally, one mechanism is associated with the two-dimensional core flow instability occurring in wide vaneless diffusers when the critical flow angle is reached, and the other mechanism is associated with the three-dimensional wall boundary layer instability occurring in the narrow diffusers.

A lot of experimental work is performed a.o. by [1-6], showing significant influence of the diffuser geometry on the vaneless diffuser performance, and also many analytical methods and theories are used to study the rotating stall phenomenon.

In the literature, different approaches have been used to investigate the rotating stall phenomenon in the vaneless radial diffusers. For example, the three-dimensional approach was applied by [7-10]. They generally hold the effect of the three-dimensional wall boundary layers near the diffuser walls responsible for the occurrence of rotating stall. On the other hand, [11-13] have used a two-dimensional approach where the effect of the wall boundary layers is not taken into account. They have applied a two-dimensional inviscid flow analysis to study the vaneless diffuser rotating stall. These studies suggest the existence of a two-dimensional core flow instability at the onset of rotating stall in the vaneless diffusers.

In this research, rotating stall instability is investigated from the point of view that it is a two-dimensional core flow instability. To reveal its flow dynamics a two-dimensional numerical model is made using the incompressible viscous flow model. The two-dimensional rotating instability similar to rotating stall is found, which is shown in [14] where the behavior and characteristics of this instability are presented.

In the first part of the paper, the numerical model is briefly described and the results for different radius ratios are presented. It is shown that the occurring number of rotating cells depends on the diffuser radius ratio and circumference. In the second part of the paper, the numerical model results are compared with results of the two-dimensional inviscid flow analysis performed by Tsujimoto et al. [13]. Here, it is shown that the two models are in good agreement. Overview of the used symbols and indices throughout the paper is given in table 1.

Table 1: Used symbols and indices

Notation	Definition
A	amplitude
D	constant for function steepness
j	imaginary number
L	diffuser length
m	number of rotating cells
N	number of impeller blades
r	radius
R	outlet-to-inlet radius ratio
t	time
u	radial velocity
v	tangential velocity
V	absolute velocity
Y	defined parameter
Greek Letters	**Definition**
α	flow angle
Ω	impeller speed
θ	circumferential position
σ	constant factor
ω	angular velocity
Subscripts	**Definition**
cr	critical
i	impeller
m	mean
s	stall
tip	impeller tip
2	diffuser inlet
3	diffuser outlet

2 Numerical model

To study the core flow instability in the vaneless radial diffuser, a two-dimensional viscous flow model of the plane parallel to the diffuser walls was developed. Here, the influence of the wall boundary layers was not taken into account, and no diffuser width was modeled.

2.1 Modeling aspects

At the diffuser outlet a constant static pressure is prescribed, assuming that the diffuser exit is connected to the space with constant pressure. At the diffuser inlet a clockwise rotating jet-wake pattern is specified. The tangential velocity component of the jet-wake pattern is constant around the circumference, and is related to the impeller tip speed as follows:

$$v = \sigma \cdot v_{tip}, \tag{1}$$

where v is the tangential velocity component, v_{tip} the impeller tip speed and σ a constant equal to 0.9. The radial velocity component of the jet-wake pattern at the diffuser inlet is described by the periodic hyperbolic tangent function:

$$u = u_m + A \cdot \frac{\tanh(D \cdot Y)}{\tanh(D)}, \tag{2}$$

where u is the radial velocity component, u_m the mean radial velocity, A the amplitude and D a constant indicating the steepness of the jet-wake function. The circumferential position θ and the impeller angular velocity ω_i, are defined within the parameter Y:

$$Y = \sin(N \cdot \theta + \omega_i \cdot t) \tag{3}$$

where t is the current time and N the number of jet-wakes around the circumference, which corresponds to the number of impeller blades.

The reference geometry and the operating conditions of the vaneless diffuser model are obtained by scaling the existing air compressor configuration at the near stall operating conditions, which is explained in [14]. The applied reference conditions of the vaneless diffuser are: $r_3/r_2 = 1.52$, $N = 17$, $\mathrm{Re} = \rho \cdot r_2 \cdot v_{tip}/\mu = 2.78 \cdot 10^6$, $v_{tip}/u_m = 9.3$, the jet-to-wake circumferential extent ratio equals 1 and the jet-to-wake radial intensity ratio equals approximately 5.5.

To perform the numerical analysis, a commercial software package FLUENT was used. Here, the governing integral equations for the conservation of mass and momentum are solved using the finite-volume approach. For discretization of the time-dependent terms the second-order implicit time integration is used, and for convection terms the QUICK scheme is used, as proposed in [15].

Although the studied flow is turbulent, the incompressible viscous flow model, with no eddy

viscosity but only molecular viscosity, is used. The current turbulence models are avoided because of the excessive numerical dissipation effect within these models. It is assumed that the two-dimensional core flow instabilities have the length scale of the prescribed jet-wake pattern at the diffuser inlet. Since turbulence models capture the diffusion-like character of turbulent mixing, associated with many small eddy structures, they damp out the solutions of large eddy structures like this one.

To mesh this geometry a simple two-dimensional quadrilateral grid consisting of 750 by 62 elements is applied. The performed calculations are unsteady and the convergence criterion of 10^{-3} , which is satisfied at each time step, is applied to the continuity, *x*-velocity and *y*-velocity residual.

2.2 Results

Using this numerical model, a two-dimensional rotating instability is obtained that is very similar to rotating stall. In figure 1 the transition from the stable operating flow condition into the fully developed two-dimensional rotating instability is shown. This transition is achieved by gradually decreasing the mean radial velocity, which corresponds to the decrease of the mass flow rate through the diffuser. The numbers #1 - #8 indicate the successive order of the pictures.

When the mean flow angle α_m, defined as $\alpha_m = \tan^{-1}(u_m/v)$, is large, the stable operating flow condition consists of a prescribed jet-wake pattern at the diffuser inlet and equally distributed alternating pattern near the diffuser outlet. The stable operating flow condition is given by image #1 in figure 1. The alternating pattern near the diffuser outlet consists of the alternating outward and reversed flow areas. The number of these regions exactly corresponds the number of prescribed jet-wakes at the diffuser inlet.

Figure 1 shows that the instability occurs when the mean flow angle at the diffuser becomes very small. When the mean flow angle becomes small, the jet-wake flow entering the diffuser space becomes able to pas underneath the alternating pattern near the diffuser outlet. This makes that the alternating pattern areas become unequal in size, which results in initiation of the two-dimensional rotating instability. This two-dimensional rotating instability fully develops within four to eight impeller revolutions, and it consists of a certain number of rotating cells that propagate with a fraction of the impeller speed. For the reference diffuser geometry and operating flow conditions it is found that 7 rotating cells occur when the instability is fully developed. These cells propagate with approximately 40 % of the impeller speed. In the absolute frame of reference, the rotating cells propagate in the same direction as the rotation direction of the impeller. Besides these similarities with the rotating stall, based on the instability characteristics, the numerical results also agree well with the measurements found in the literature for the same type of diffusers, which is shown in [16]. Because of the similarity with the rotating stall phenomenon and good agreement with the measurements found in the literature, it is believed that this instability might contribute to the vaneless diffuser rotating stall.

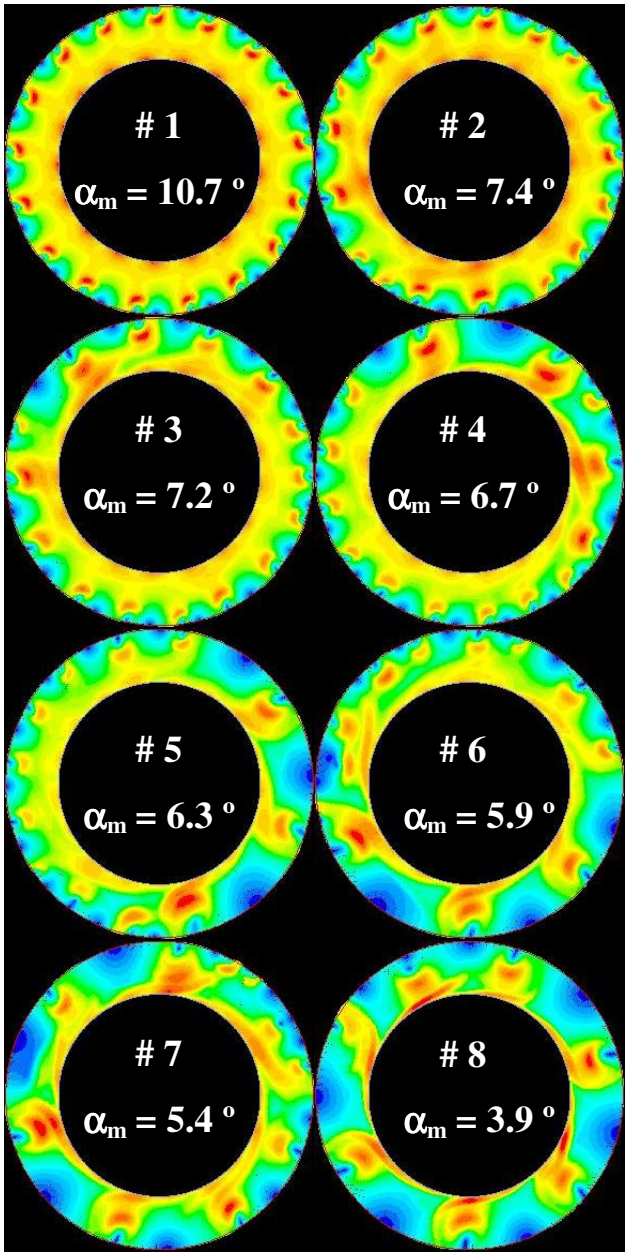

Fig.1: The development of the instability

To investigate the influence of the diffuser radius ratio, $R = r_3/r_2$, on the two-dimensional rotating instability, the diffuser outlet radius is varied while the inlet radius remained unchanged. The diffuser radius ratios of 1.2, 1.52 and 2.0 were investigated. In figure 2, solutions of the stable and unstable operating flow condition are given, corresponding to the three different diffuser radius ratios. Figure 2 shows that not only the number of rotating cells but also their size changes as the diffuser radius ratio is varied. The number of rotating cells decreases with increasing diffuser ratio, while the size of the cells increases.

This influence of the diffuser radius ratio can be explained as follows. As the diffuser radius ratio increases, the diffuser length, $L = r_3 - r_2$, becomes larger, which allows the cells to become larger in their radial extent. It seems that the circumferential and radial extent of the rotating cells tend to be proportional, which means that the diffuser length is most likely the determinative parameter for the size of the rotating cells.

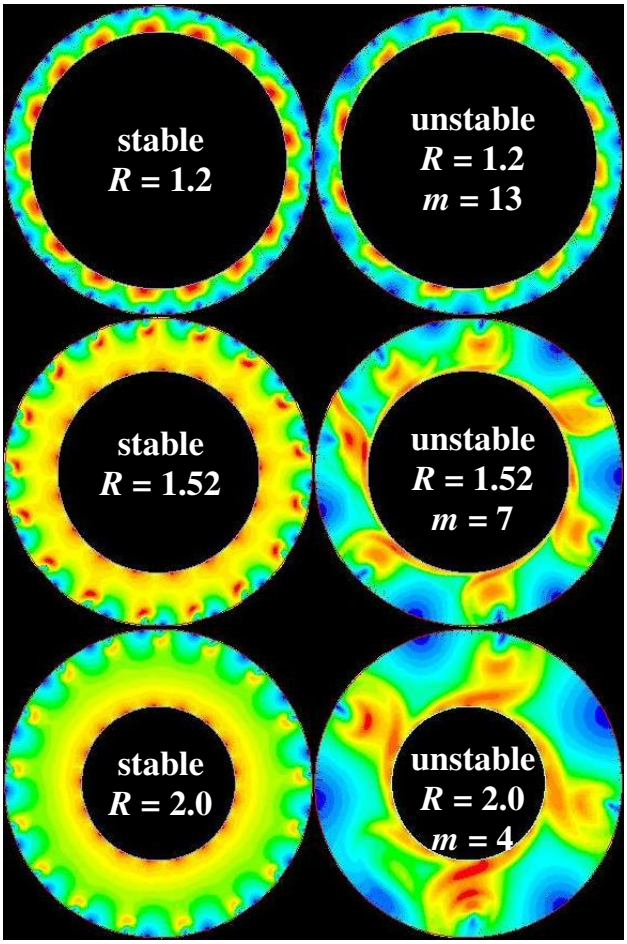

Fig.2: Influence of the diffuser radius ratio

Since the size of the rotating cells is most likely defined by the diffuser length, the maximum number of the cells is then probably defined by the diffuser circumference. The number of cells of a given size that fits into the diffuser is most likely limited by its circumference. Therefore, the maximum number of the cells, occurring when the two-dimensional rotating instability is fully developed, can be estimated by half the ratio between the circumference and the diffuser length:

$$m = \frac{1}{2} \cdot \frac{\pi \cdot (r_3 + r_2)}{r_3 - r_2} \qquad (4)$$

Because each rotating cell is accompanied by an additional vortex of the opposite rotation direction and of approximately the same size, this needs to be included in the estimation. In order to take the space between the rotating cells into account, the ratio between the circumference and the diffuser length is divided by factor 2.

Using equation (4), the maximum number of rotating cells that can occur in the vaneless diffusers of radius ratio 1.2, 1.52 and 2.0 is estimated to be 17.3, 7.6 and 4.7 respectively. Since the value of m is an integer number, the estimated number of rotating cells for the diffuser radius ratios of 1.2, 1.52 and 2.0 is adapted to 17-18, 7-8 and 4-5 respectively. In figure 2 it is shown that m = 13 for R = 1.2, m = 7 for R = 1.52 and m = 4 for R = 2. With this observation it seems that the maximum number of rotating cells is well predicted for R = 1.52 and R = 2. The obtained number of rotating cells for R = 1.2 approaches the estimated value, but is not exactly the same. This is probably due to the very small distance between the outlet boundary condition and the diffuser inlet, which leads to a somewhat suppressed solution that makes this comparison difficult and uncertain.

The observed number of rotating cells in figure 2 that was compared with equation (4), is in all cases the maximum occurred number of rotating cells. The maximum occurring number of rotating cells, is being considered as a fully developed condition of instability. Just after the stability limit is reached, the number of rotating cells rapidly grows towards the maximum number that fits into the diffuser geometry, as shown in figure 1.

When continuing to decrease the mass flow rate through the diffuser after the maximum number of cells is reached, the number of rotating cells starts to decrease with further decrease of the mass flow rate. This is shown in figure 3, where the numbers #1 - #4 indicate the successive order of the pictures. This

means that the diffuser length is not the only parameter influencing the number of rotating cells, but it is together with the mass flow rate, decisive for the occurring number of rotating cells.

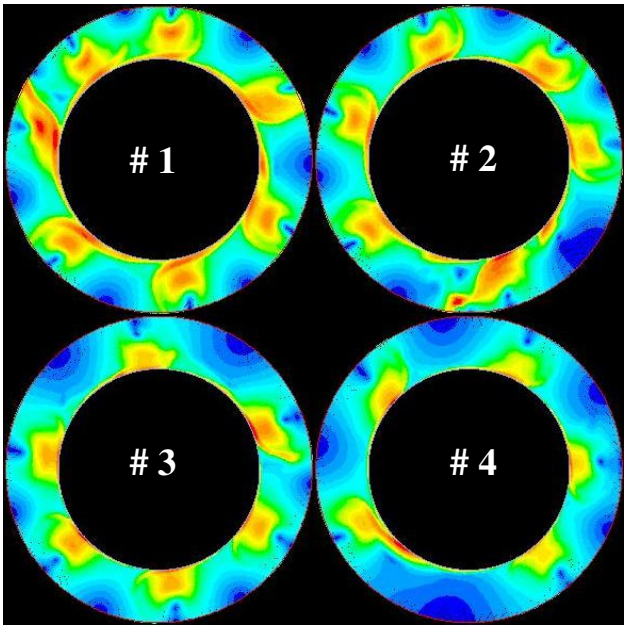

Fig.3: Decrease of the number of cells with decreasing mass flow rate

The influence of the diffuser radius ratio on the critical flow angle, the number of rotating cells and their propagation speed, as obtained by the two-dimensional numerical model, is given in figures 4 and 5.

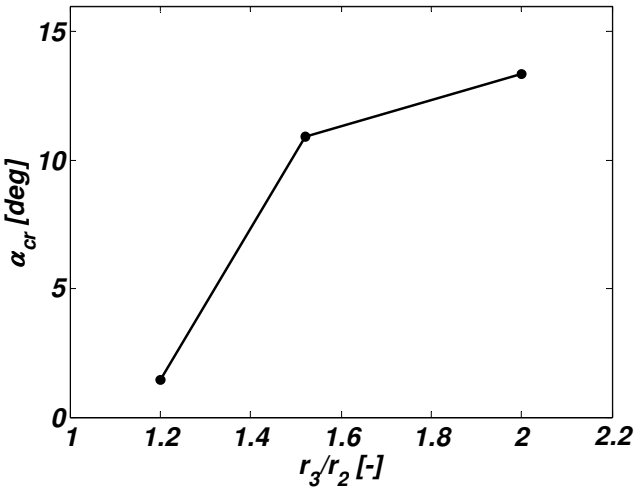

Fig.4: Critical flow angle versus radius ratio

The critical flow angle is found to be strongly dependent on the diffuser radius ratio. Figure 4 shows that when the diffuser radius ratio decreases, the critical flow angle also decreases and the core flow stability of the vaneless diffuser improves. Figure 5 shows that not only the number of rotating cells but also their propagation speed decreases with increasing diffuser radius ratio. In figure 5, the maximum occurred number of rotating cells for each diffuser radius ratio is connected with a solid line. The number of rotating cells obtained when the mass flow rate is further decreased, after the fully developed condition of instability is reached, is also given. The mass flow rate was continuously decreased until it has reached the final value of zero. The arrows point in the direction of the mass flow decrease. Note that for constant diffuser radius ratio, the propagation speed of the cells does not change with changing number of rotating cells.

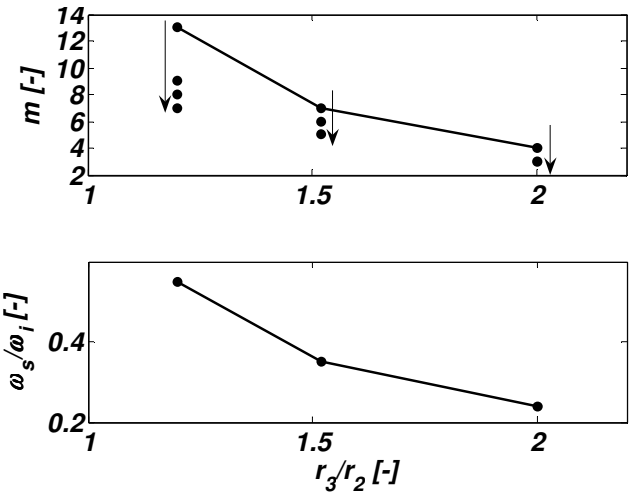

Fig.5: Number of cells and their propagation speed versus radius ratio

3 Two-dimensional inviscid model

Similar model to the numerical model described above was developed by Tsujimoto et al. [13]. They have performed a linear two-dimensional inviscid analysis to study the rotating stall instability in vaneless diffuser space. Here, rotating stall is studied from the point of view that can be a two-dimensional inviscid flow instability under the boundary conditions of vanishing velocity disturbance at the diffuser inlet and of vanishing pressure disturbance at the diffuser outlet. It is assumed that the flow is inviscid and incompressible and that the disturbance is small enough to allow linear analysis.

In this two-dimensional inviscid flow analysis a constant pressure is prescribed at the diffuser outlet. At the diffuser inlet, the unsteady flow field in the vaneless diffuser space is represented by the velocity induced by vorticity and the two additional potential flow components. The unsteady components are given by a general complex representation,

$$u = \tilde{u}(r)\exp\{j(\omega \cdot t - m \cdot \theta)\} \quad (5)$$

$$v = \tilde{v}(r)\exp\{j(\omega \cdot t - m \cdot \theta)\} \quad (6)$$

where j is the imaginary number, t the time, ω the angular frequency and m the number of rotating cells. For more detail about the modeling conditions within this two-dimensional inviscid analysis see reference [13].

Tsujimoto et al. [13] have found that the flow instability similar to vaneless diffuser rotating stall may occur even with uniform outward flow. Their linear stability analysis shows that the critical flow angle and the propagation speed are functions of only the diffuser radius ratio.

This two-dimensional analysis is similar to the numerical model in the sense that they are both two-dimensional, incompressible and have constant pressure at the diffuser outlet. The major differences between the two models lie in the prescribed inlet flow conditions. In the two-dimensional inviscid flow analysis a rotating uniform velocity profile with the assumed number of modes is prescribed, while in the numerical model a rotating jet-wake with 17 impeller blades is prescribed. In the case of the two-dimensional inviscid flow analysis the number of rotating cells is prescribed, while in the numerical model this value is an outcome based on the modeling conditions.

Because of the strong similarity between the two models, but also because of the slightly different approach to the rotating stall instability, it is interesting to comparre the results of these two models. In the following section, the results obtained by the numerical model are compared with the results of this linear two-dimensional inviscid flow analysis.

4 Comparison

In this section, the results presented in figures 4 and 5 are compared with the results of the two-dimensional inviscid flow analysis. Tsujomoto et al. [13] have performed the two-dimensional inviscid flow analysis only for the lower order modes, namely only m = 1, 2 and 3. Because in the current numerical model higher numbers of rotating cells were obtained, the solution for the higher order modes in the two-dimensional inviscid analysis is desired for comparison. In this paper, the higher order mode solutions of the two-dimensional inviscid flow analysis are calculated and presented. These higher order mode solutions are given in figures 6 and 7, together with the low order mode solutions as determined in [13]. In figure 6 the critical flow angle is plotted versus the diffuser radius ratio, and in figure 7 the propagation speed is plotted versus the diffuser radius ratio for m = 1-13.

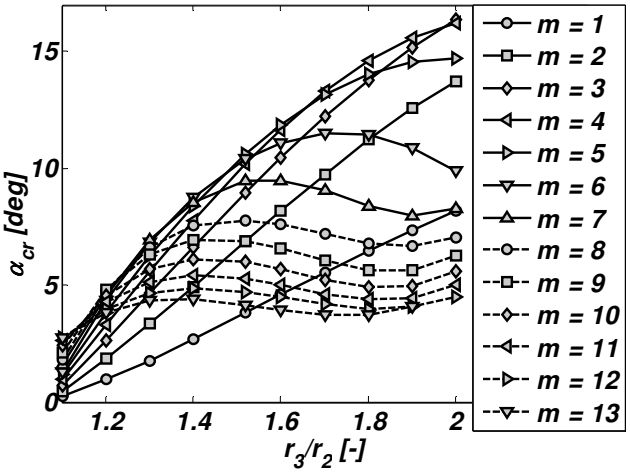

Fig.6: Critical flow angle obtained by the two-dimensional inviscid flow model

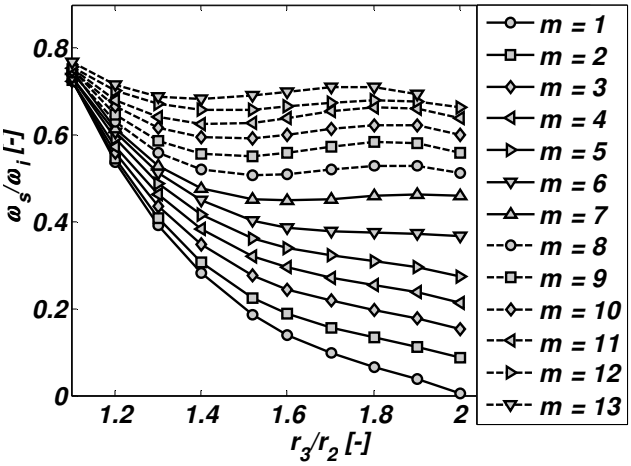

Fig.7: Propagation speed obtained by the two-dimensional inviscid flow model

Figure 6 shows that for each mode the critical flow angle first increases with increasing diffuser radius ratio and then starts to decrease as the diffuser radius ratio becomes higher. This transition from positive to negative slope of the curve occurs sooner for the higher order modes than for the lower order modes. Since the critical flow angle should increase with increasing diffuser radius ratio according to many experimental observations in the literature, as shown in [16], the decrease of the critical flow angle is not considered to have any physical significance.

Considering the modes on the positive slope of the curves as existent modes, and the modes on the negative slope of the curve as non-existing, it follows that for lower R up to higher order modes are existent than for higher R, where $R = r_3/r_2$.

According to this two-dimensional inviscid analysis, the existent modes m = 1-18 correspond to R = 1.2, modes m = 1-7 to R = 1.52, and modes m = 1-4 to R = 2. Since the maximum order mode obtained at each diffuser radius ratio comes nearest to the non-existing modes, it is being considered as the most unstable mode occurring for that particular diffuser geometry. The maximum order modes obtained at each diffuser radius ratios are therefore also expected to occur first when the diffuser flow becomes unstable.

The maximum order modes or the most unstable modes obtained by the two-dimensional inviscid flow analysis are compared with the first occurring mode numbers after the instability inception obtained by the numerical model. Since the first occurring mode numbers obtained by the numerical model are, m = 13 for R = 1.2, m = 7 for R = 1.52 and m = 4 for R = 2, a good agreement is found between the two models. This comparison is illustrated in figure 8, where the most unstable modes are plotted versus the diffuser radius ratio. Generally, the same growing trend of the mode number is obtained as the diffuser radius ratio decreases. For the diffuser radius ratio R = 1.52 and higher, the same number of cells is obtained by both models.

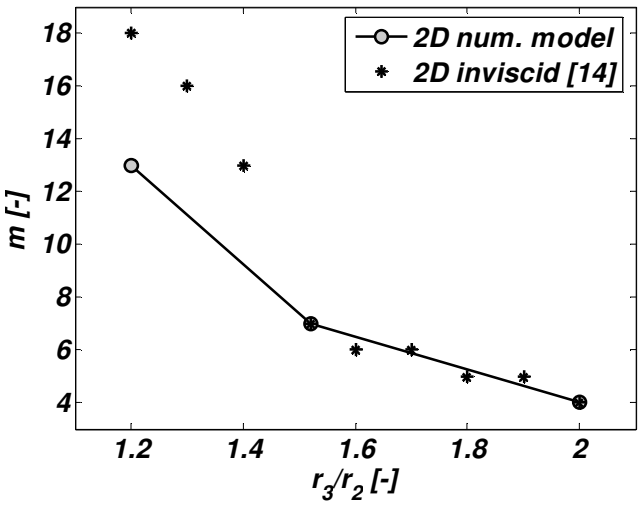

Fig.8: Comparison of the obtained mode numbers between the two models

The critical flow angles from figure 6 and the propagation speeds from figure 7, corresponding to the maximum mode number for a given diffuser radius radio, are also compared with the critical flow angles and propagation speeds obtained by the numerical model. In figure 9, the critical flow angles and the propagation speed of the cells, obtained by the two models, are compared for different diffuser radius ratios.

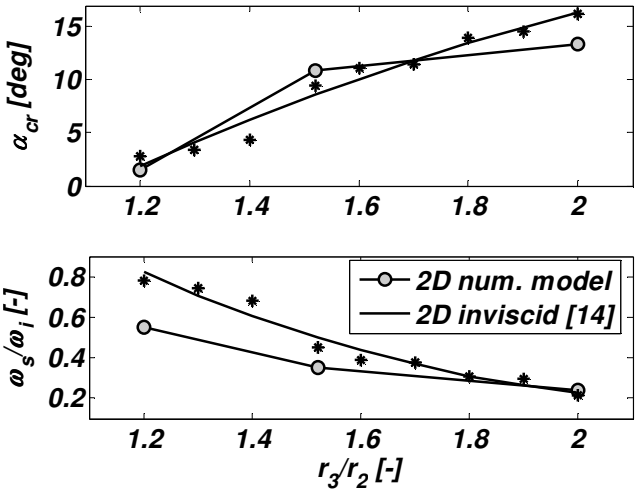

Fig.9: Comparison of the critical flow angles and the propagation speeds between the two models

To indicate the changing trend obtained by the two-dimensional inviscid flow analysis, a polynomial is fitted through the obtained values, while the values obtained by the numerical model are connected with the solid line. This figure shows that not exact but quite good agreement between the two models is obtained.

5 Conclusion

A two-dimensional viscous incompressible flow model was developed to study the core flow instability within the wide vaneless radial diffusers of centrifugal compressors. With this numerical model of the vaneless diffuser core flow, a two-dimensional rotating instability similar to rotating stall in vaneless diffusers was found to exist.

The two-dimensional rotating instability occurs when the critical flow angle is exceeded. It fully develops within a few impeller revolutions and it consists of a number of rotating cells that propagate with a fraction of the impeller speed.

It is shown that the number of rotating cells and their size change with the diffuser geometry, and that the maximum number of rotating cells, occurring when the two-dimensional rotating instability is fully developed, can be estimated. The estimation is based on the diffuser space length and the diffuser circumference.

Similar approach for the study the rotating stall in vaneless radial diffusers is used by Tsujimoto et al. [13], who have performed a two-dimensional inviscid flow analysis in the vaneless diffuser space. Since they have presented the solutions only for low order mode numbers, m = 1-3, the solutions for the higher order modes, m = 1-13, were also obtained

and presented in this paper. The higher order mode solutions of the two-dimensional inviscid flow analysis were interesting to compare with the current numerical model, because with this model higher order modes were obtained. It is shown that the numerical results are in good agreement with the two-dimensional inviscid flow model. The two-dimensional inviscid flow model shows that the maximum mode number, considered as the most unstable mode, decreases with increasing diffuser radius ratio, which is in good agreement with the number of modes obtained by the numerical model. The same maximum number of cells for the most diffuser radius ratios was obtained by both models, and the obtained critical flow angles and the propagation speeds of the rotating cells with the two models were also in good agreement.

Good agreement between the current numerical model and the two-dimensional inviscid flow analysis performed in [13], is very supportive to the both models, and to the two-dimensional approach used for the study of rotating stall instability in the vaneless radial diffusers.

Acknowledgements:
Prof. Yoshinobu Tsujimoto is thanked for clarifying the two-dimensional inviscid flow analysis in [13]. TNO from Delft is thanked for their guidance in this project.

References:

[1] Abdelhamid, A. N., and Bertrand, J., Distinctions between Two Types of Self-Excited Gas Oscillations in Vaneless Radial Diffusers, *ASME Paper* 79-GT-58*, Canadian Aeronautics and Space J*, Vol.26, 1980, pp. 105-117.

[2] Dou, H. -S., Investigation of the Prediction of Losses in Radial Vaneless Diffusers, *ASME Paper* 91-GT-323, 1991.

[3] Shin, Y. H., Kim, K. H., and Son, B. J., An Experimental Study on the Development of a Reverse Flow Zone in a Vaneless Diffuser, *JSME International J*, Vol.41, series B, 1998, pp.546-555.

[4] Abdelhamid, A. N., Effects of Vaneless Diffuser Geometry on Flow Instability in Centrifugal Compression Systems, *Canadian Aeronautics and Space Journal,* Vol.29, No.3, 1983, pp. 259-266.

[5] Frigne, P. and Van den Braembussche, R., Distinction between different types of impeller and diffuser roatating stall in a centrifufgal compressor with vaneless diffuser, *ASME Journal of Engineering for Gas Turbines and Power*, Vol.106, No.2, pp., 1984, pp. 468-474.

[6] Kinoshita, Y. and Senoo, Y, Rotating Stall Induced in Vaneless Diffusers of Very Low Specific Speed Centrifugal Blowers, *ASME Journal of Engineering for Gas Turbines and Power*, Vol.107, 1985, pp. 514-521.

[7] Jansen, W., Rotating Stall in a Radial Vaneless Diffuser, *ASME J of Basic Engineering*, Vol.86, 1964, pp. 750-758.

[8] Senoo, Y., and Kinoshita, Y., Influence of Inlet Flow Conditions and Geometries of Centrifugal Vaneless Diffusers on Critical Flow Angle for Reverse Flow, *ASME J of Fluids Engineering*, Vol.99, 1977, pp. 98-103.

[9] Frigne, P., and Van den Braembussche, R., A Theoretical Model for Rotating Stall in the Vaneless Diffuser of a Centrifugal Compressor, *ASME J of Engineering for Gas Turbines and Power*, Vol.107, 1985, pp. 507-513.

[10] Dou, H. –S., and Mizuki, S., Analysis of the Flow in Vaneless Diffusers with Large Width-to-Radius Ratio, *ASME J of Turbomachinery*, Vol.120, 1998, pp. 193-201.

[11] Abdelhamid, A.N., Analysis of Rotating stall in Vaneless Diffusers of Centrifugal Compressors, *ASME Paper* 80-GT-184, 1980.

[12] Moore, F. K., Weak Rotating Flow Disturbances in a Centrifugal Compressor With a Vaneless Diffuser, *ASME Journal of Turbomachinery,* Vol.111, 1989, pp. 442-449.

[13] Tsujimoto, Y., Yoshida, Y., and Mori, Y., Study of Vaneless Diffuser Rotating Stall Based on Two-Dimensional Inviscid Flow Analaysis, *ASME J of Fluids Engineering*, Vol.118, 1996, pp. 123-127.

[14] Ljevar, S., de Lange, H. C., and van Steenhoven, A. A., Two-Dimensional Rotating Stall Analysis in a Wide Vaneless Diffuser, *International Journal of Rotating Machinery*, Vol.12, 2006, pp. 1-11.

[15] Leonard, B.P., A Stable and Accurate Convective Modeling Procedure Based on Quadratic Upstream Interpolation, *Comp Meth Appl Mech* , Vol.19, 1979, pp. 59-98.

[16] Ljevar, S., de Lange, H. C., and van Steenhoven, A. A., Rotating Stall Characteristics in a Wide Vaneless Diffuser, *Proc. ASME Turbo Expo 2005, Reno-Tahoe, Nevada, USA*, Vol.6, part B, 2005.